Inorganic Chemistry

ARTICLE

pubs.acs.org/IC

# Triggered Dye Release via Photodissociation of Nitric Oxide from Designed Ruthenium Nitrosyls: Turn-ON Fluorescence Signaling of Nitric Oxide Delivery

Nicole L. Fry, Julia Wei, and Pradip K. Mascharak*

Department of Chemistry and Biochemistry, University of California, Santa Cruz, California 95064, United States

Supporting Information

**ABSTRACT:** Two new fluorescein-tethered nitrosyls derived from designed tetradentate ligands with carboxamido-N donors have been synthesized and characterized by spectroscopic techniques. These two diamagnetic {Ru-NO}$^6$ nitrosyls, namely, [($Me_2$bpb)Ru(NO)(FlEt)] (**1-FlEt**, $Me_2$bpb = 1,2-bis(pyridine-2-carboxamido)5-dimethylbenzene, **FlEt** = fluorescein ethyl ester) and [(($OMe)_2$IQ1)Ru(NO)(FlEt)] (**2-FlEt**, $(OMe)_2$-IQ1 = 1,2-bis(isoquinoline-1-carboxamido)-4,5-dimethoxybenzene), display NO stretching frequencies ($\nu_{NO}$) at 1846 and 1832 $cm^{-1}$ in addition to their FlEt carbonyl stretching frequencies ($\nu_{CO}$) at 1715 and 1712 $cm^{-1}$, respectively. Coordination of the dye ligand enhances the absorptivity and NO photolability of these two nitrosyls in the visible region (450−600 nm) of light. Exposure to visible light promotes rapid loss of NO from both {Ru-NO}$^6$ nitrosyls to generate Ru(III) photoproducts in dry aprotic solvents, such as MeCN and DMF. The $FlEt^-$ moiety remains bound to the paramagnetic Ru(III) center in such cases, and hence, the photoproducts exhibit very weak fluorescence from the dye unit. In the presence of water, the Ru(III) photoproducts undergo further aquation and loss of the $FlEt^-$ moiety via protonation. These steps lead to turn-ON fluorescence (from the free FlEt unit) and provide a visual signal of the NO photorelease from **1-FlEt** and **2-FlEt** in aqueous media.

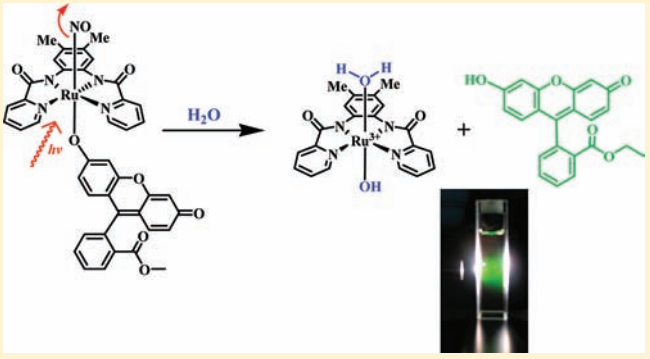


## INTRODUCTION

In recent years, the role of nitric oxide (NO) in biological systems has been elucidated in detail.[1−4] It is now known that this small gaseous signaling molecule can greatly affect its physiological response depending on its concentration. For example, nanomolar concentrations of NO affect vasodilatation of smooth muscles[1,5] and neurotransmission in the brain.[2] In contrast, elevated NO concentrations in the micromolar range are employed by macrophages to eliminate pathogens.[6,7] In addition, high NO concentrations can lead to apoptosis (programmed cell death).[8−10] This latter finding suggests that malignant cells can be destroyed via exposure to a high flux of NO. Such an expectation has been realized in recent studies where cancers of different grades and origins have been eradicated via NO-induced apoptosis.[8−10] These results have prompted intense research activity in the area of development of designed NO donors for selective delivery of NO to malignant locales.[11]

Certain transition metals (Fe,[12] Mn,[13] and Ru[14]) can tightly bind NO, forming metal nitrosyls that release NO upon exposure to specific wavelengths of light. Such metal nitrosyls could provide a way to deliver NO to selected sites as a new type of photodynamic therapy (PDT).[15] Ruthenium nitrosyls are preferable for biological use due to their inherent stability in aqueous media compared to iron and manganese nitrosyls.[16] However, ruthenium nitrosyls with simple ligands (such as $NH_3$ and Cl)[17,18] release NO only upon exposure to UV light, which itself could also harm the biological target. Careful design of more complex ligand frames has recently allowed one to overcome this obstacle.[19] In our synthetic strategy, beginning with the tetradentate dicarboxamide ligand frame ($H_2$bpb),[20] addition of electron-donating substituents on the phenylenediamine ring ($H_2Me_2$bpb[20] and $H_2(OMe)_2$bpb[21]) and exchange of the pyridine units for quinoline moieties ($H_2Me_2$bQb,[20] $H_2(OMe)_2$bQb,[22] $H_2$(OMe)IQ1[21]) have so far resulted in ligands that promote visible light absorption by the corresponding ruthenium nitrosyls. For example, [(bpb)Ru(NO)(Cl)][20] releases NO upon exposure to UV light (absorption maximum, $\lambda_{max}$ = 395 nm), whereas [(($OMe)_2$bQb)Ru(NO)(Cl)][22] exhibits moderate NO release when exposed to visible light ($\lambda_{max}$ = 500 nm). To further increase the efficiency of NO release with visible light, we have employed a directly coordinated dye choromophore to improve the extent of visible light absorption. Indeed, the quantum yield at 500 nm ($\phi_{500}$) of NO release is increased from 0.0008 for [($Me_2$bpb)Ru(NO)(Cl)] to 0.052 for

**Received:** June 9, 2011
**Published:** August 04, 2011

[$(Me_2bpb)Ru(NO)(Resf)$] (**1-Resf**), in which the dye resorufin (Resf) is bound to the Ru center.[22]

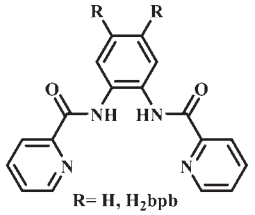


R= H, $H_2bpb$
R= Me, $H_2Me_2bpb$
R= OMe, $H_2(OMe)_2bpb$

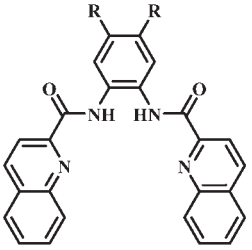


R = Me, $H_2Me_2bQb$
R = OMe, $H_2(OMe)_2bQb$

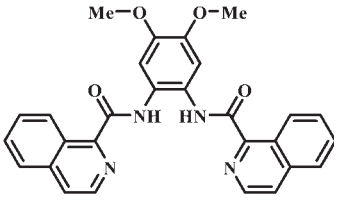


$H_2(OMe)_2IQ1$

Free resorufin is also a very efficient fluorophore that exhibits red fluorescence upon light exposure. Although the fluorescence of the free dye is partly quenched when Resf is directly attached to the Ru center of the $\{RuNO\}^6$ nitrosyls, the residual fluorescence of **1-Resf** is enough to visualize the complex in cellular matrixes.[22] This allowed us to track the NO donor within the biological targets. To extend this concept further and develop new trackable NO donors, we chose fluorescein as the next chromophore. Fluorescein is a green fluorescent dye commonly used for biological studies.[23,24] Ford and co-workers have recently shown that attachment of a fluorescein dye derivative provides fluorescence and moderate enhancement of the NO photolability of a iron sulfur nitrosyl compound (Roussin's red salt).[25] However, the fluorescein dye in this compound was attached to bridging S atom(s) through a $(CH_2)_2$ linker. We were interested to see how the *direct* attachment of fluorescein to the Ru center of our designed ruthenium nitrosyls would affect the fluorescence and NO photolability of the resulting nitrosyls upon exposure to 500 nm light. In this account, we report the syntheses and spectroscopic properties of two new $\{RuNO\}^6$ nitrosyls with ligated fluorescein ethyl ester dye (**FlEt**), namely, [$(Me_2bpb)Ru(NO)(FlEt)$] (**1-FlEt**, $Me_2bpb$ = 1,2-bis-(pyridine-2-carboxamido)-4,5-dimethylbenzene) and [$((OMe)_2$-IQ1)$Ru(NO)(FlEt)$] (**2-FlEt**, $(OMe)_2IQ1$ = 1,2-bis(isoquinoline-1-carboxamido)-4,5-dimethoxybenzene). Investigation of the fluorescent properties and NO photolability of these two complexes reveal that both nitrosyls exhibit *turn-ON* fluorescent signals triggered by photodissociation of NO upon exposure to 500 nm light.

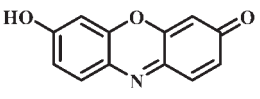


Resorufin

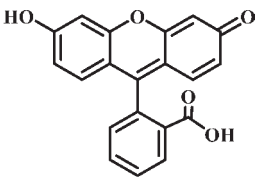


Fluorescein

**[$(Me_2bpb)Ru(NO)(FlEt)$] (1-FlEt)**

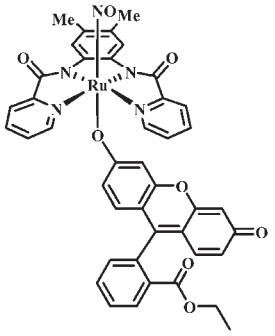


**[$((OMe)_2IQ1)Ru(NO)(FlEt)$] (2-FlEt)**

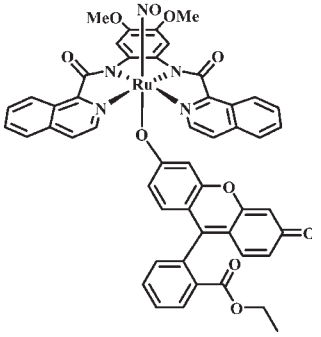


## EXPERIMENTAL SECTION

**Materials and General Procedures.** NO gas was purchased from Spectra Gases Inc. and was purified by passing through a long KOH column prior to use. $RuCl_3 \cdot xH_2O$ (Aldrich Chemical Co.) was treated several times with concentrated HCl to prepare the starting metal salt, $RuCl_3 \cdot 3H_2O$. Fluorescein and $AgBF_4$ were purchased from Fluka and Alfa-Aesar, respectively. All solvents were dried by standard techniques and distilled prior to use. The starting complexes [$(Me_2bpb)$-$Ru(NO)(Cl)$][20] and [$((OMe)_2IQ1)Ru(NO)(Cl)$][21] were synthesized by following procedures reported by us previously. The published procedure for fluorescein ethyl ester[25] was modified to obtain high yields of the pure dye. All other chemicals were purchased from Aldrich Chemical Co. and used without further purification.

**Syntheses of Compounds.** *Fluorescein Ethyl Ester (**FlEt**).* A slurry of fluorescein (1.00 g, 3.01 mmol) in 150 mL of EtOH was treated with 7 mL of sulfuric acid and heated to reflux temperature for 20 h in a 500 mL round-bottom flask covered with aluminum foil. EtOH was then removed via rotary evaporation, leaving a bright yellow oil. The product was extracted into dichloromethane (DCM) via liquid−liquid extraction using DCM and water, and the DCM layer was washed with sodium bicarbonate (2.50 g, 30.00 mmol) dissolved in 50 mL of water. Finally, DCM was removed via rotary evaporation, leaving a red-orange solid. Yield: 0.97 g (90%). Selected IR frequencies (KBr disk, in $cm^{-1}$): 1718 (m), 1640 (m), 1595 (vs), 1495 (s), 1460 (vs), 1384 (s), 1263 (vs), 1205 (s), 1107 (s). $^1H$ NMR in $CDCl_3$, $\delta$ from TMS: 8.72 (d, 1H), 7.74 (t, 1H), 7.69 (t, 1H), 7.33 (d, 1H), 6.99 (d, 2H), 6.89 (s, 2H), 6.81 (d, 2H), 4.01 (q, 2H), 0.92 (t, 3H).

*[$(Me_2bpb)Ru(NO)(FlEt)$] (**1-FlEt**).* A solution of 0.150 g of [$(Me_2bpb)Ru(NO)(Cl)$] (0.294 mmol) was prepared in 20 mL of MeCN and treated with $AgBF_4$ (0.057 g, 0.294 mmol). A separate solution of 0.106 g of **FlEt** (0.294 mmol) in 20 mL of MeCN was treated with NaH (0.007 g, 0.294 mmol). Both solutions were then heated to reflux temperature, and the **FlEt** solution was slowly added to the [$(Me_2bpb)Ru(NO)(Cl)$] solution with stirring. Heating of the mixture (with constant stirring) was continued at reflux temperature for 5 h. Next, the bright red solution was cooled to −20 °C for 1 h to allow full precipitation of impurities, which were filtered off using a Celite pad. The filtrate was condensed to half the original volume, 5 mL of $Et_2O$ was added, and then it was stored at −20 °C for 48 h. The red precipitate was filtered, washed several times with $Et_2O$, and dried in vacuo. It was finally recrystallized from $CHCl_3$. Yield: 0.100 g (41%). Anal. Calcd for $C_{42}H_{31}N_5O_8Ru$ (**1-FlEt**): C, 60.43; H, 3.74; N, 8.39. Found: C, 60.35; H, 3.49; N, 8.44. Selected IR frequencies (KBr disk, in $cm^{-1}$): 1846 (s), 1715 (m), 1635 (s), 1578 (vs), 1473 (s), 1379 (m), 1273 (s), 1206 (m), 1104 (m). $^1H$ NMR in $CDCl_3$, $\delta$ from TMS: 8.83 (d, 2H), 8.39 (s, 2H), 3.32 (d, 1H), 8.28 (d, 1H), 8.24 (t, 1H), 8.21 (t, 1H), 8.16 (d, 1H), 7.79 (t, 1H), 7.76 (t, 1H), 7.64 (t, 1H), 7.60 (t, 1H), 7.17 (d, 1H), 6.77


dx.doi.org/10.1021/ic201242d |*Inorg. Chem.* 2011, 50, 9045–9052

(d, 1H), 6.49 (d, 1H), 6.39 (d, 1H), 6.30 (s, 1H), 5.81 (d, 1H), 5.74 (s, 1H), 3.98 (q, 1H), 3.89 (q ,1H), 2.27 (s, 6H), 0.84 (t, 3H). ESI-MS: $m/z$ 836 ($M^+$). UV−vis in MeCN, $\lambda_{max}$ in nm ($\varepsilon$ in $M^{-1}$ $cm^{-1}$): 270 (25 500), 375 (11 000), 450 sh (18 500), 475 (24 000), 510 sh (20 100).

*[((OMe)$_2$IQ1)Ru(NO)(FlEt)]* (***2-FlEt***). A batch of [((OMe)$_2$IQ1)-Ru(NO)(Cl)] (0.150 g, 0.233 mmol) was treated with $AgBF_4$ (0.045 g, 0.233 mmol) in 15 mL of MeCN and heated to reflux temperature. Meanwhile, a slurry of **FlEt** (0.084 g, 0.233 mmol) was treated with 1 equiv of NaH (0.006 g, 0.233 mmol) in MeCN and also brought to reflux temperature. The hot **FlEt** solution was then added to the [((OMe)$_2$IQ1)Ru(NO)(Cl)] solution, and the mixture was kept at reflux temperature for 8 h. Over the course of the reaction, a red-orange precipitate separated out. The precipitate was collected by filtration and recrystallized from $CHCl_3$/pentane. Yield: 0.172 g (76%). Anal. Calcd for $C_{50}H_{35}N_5O_{10}Ru$ (**2-FlEt**): C, 62.11; H, 3.65; N, 7.24. Found: C, 62.17; H, 3.50; N, 7.42. Selected IR frequencies (KBr disk, in $cm^{-1}$): 1832 (m), 1712 (w), 1617 (vs), 1579 (vs), 1496 (s), 1332 (m), 1287 (s), 1213 (w), 1097 (s). $^1$H NMR in $CDCl_3$, $\delta$ from TMS: 10.339 (d, 1H), 10.193 (d, 1H), 8.790 (dd, 2H), 8.521 (s, 1H), 8.482 (s, 1H), 8.141 (m, 3H), 7.996 (tt, 3H), 7.891 (dt, 2H), 7.809 (t, 1H), 7.596 (dt, 2H), 7.054 (d, 1H), 6.703 (d, 1H), 6.440 (d, 1H), 6.293(d, 1H), 6.057 (s, 1H), 5.875 (d, 1H), 5.363 (s, 1H), 4.012 (s, 3H), 3.994 (s, 3H), 3.885 (q, 1H), 3.796 (q, 1H), 0.701 (t, 3H). ESI-MS: $m/z$ 968 (M+). UV−vis in MeCN, $\lambda_{max}$ in nm ($\varepsilon$ in $M^{-1}$ $cm^{-1}$): 280 (28 700), 320 sh (17 000), 365 sh (10 200), 450 sh (21 00), 475 (28 000), 510 sh (22 700).

**Physical Measurements.** The $^1$H NMR spectra were recorded at 298 K on a Varian Inova 500 MHz instrument. A PerkinElmer Spectrum-One FT-IR spectrometer was used to monitor the IR spectra of the complexes. The electronic absorption spectra were obtained with a scanning Cary 50 spectrophotometer (Varian Associates). Fluorescence spectra were recorded with a PerkinElmer LS50B fluorescence/luminescence spectrometer. X-band electron paramagnetic resonance (EPR) spectra were obtained with a Bruker ELEXSYS 500 spectrometer at 125 K. Electrospray ionization mass spectrometry (ESI-MS) was carried out on a Waters Micromass ZMD mass spectrometer. Release of NO upon illumination in aqueous solution was monitored by using the *in*NO Nitric Oxide Monitoring System (Innovative Instruments Inc.) fitted with an *ami*-NO 2008 electrode. The NO amperograms were recorded using stirred solutions contained in open vials.

**Photolysis Experiments.** The quantum yield ($\phi$) values of NO release were obtained using a tunable Apex Illuminator (150 W xenon lamp) equipped with a Cornerstone 130 1/8 M monochromator (measured intensity of ∼10 mW). Actinochrome N (475/610) was used to as the standard for the quantum yield values calculated at 500 nm ($\phi_{500}$).[26] Solutions of **1-FlEt** and **2-FlEt** were prepared and placed in 2 × 10 mm quartz cuvettes, 1 cm away from the light source. All solutions were prepared to ensure sufficient absorbance (>90%) at the irradiation wavelength, and changes in electronic spectrum at 750 and 700 nm for **1-FlEt** and **2-FlEt**, respectively (<10% photolysis), were used to determine the extent of photorelease of NO.

**Fluorescence Experiments.** Fluorescence spectra were recorded with a PerkinElmer LS50B fluorescence/luminescence spectrometer. All samples were prepared in four-sided 1 cm × 1 cm quartz cuvettes such that the absorbance was <0.1 at the excitation wavelength. Fluorescence quantum yields were determined relative to fluorescein in 0.1 N NaOH ($\phi$ = 0.95).[27] The concentration of the reference was adjusted to match the absorbance of the test sample at the excitation wavelength (480 nm). The fluorescence intensity of the resulting fluorescence spectra was integrated from 500 to 650 nm for comparison. Fluorescence turn-ON measurements of **1-FlEt** and **2-FlEt** were obtained upon comparison of samples kept in the dark or exposed to visible light (1 min intervals) from an IL 410 Illumination System from Electro-FiberOptics Corp. (halogen lamp) equipped with a $\lambda \geq$ 465 nm cutoff filter (measured intensity = 300 mW).

## RESULTS AND DISCUSSION

**Synthesis.** To synthesize a fluorescein-bound ruthenium nitrosyl, the structure of the dye molecule had to be considered. For example, fluorescein has a phenolato-O as well as a carboxylato-O donor center, both of which are capable of binding to the metal center. Indeed, initial attempts to combine fluorescein with our designed ruthenium nitrosyls resulted in a mixture of products. To circumvent this problem, we decided to protect one of the metal binding sites of the fluorescein dye. Simple treatment of fluorescein with concentrated sulfuric acid in ethanol resulted in conversion of the carboxylic acid into an ethyl ester, thus leaving only the phenolato-O donor available for metal binding. Removal of the chloride from [(Me$_2$bpb)Ru(NO)(Cl)] (**1-Cl**) with $AgBF_4$ in MeCN allowed the fluorescein ethyl ester (**FlEt**, deprotonated with NaH) to bind the Ru center, affording [(Me$_2$bpb)Ru(NO)(FlEt)] (**1-FlEt**) in good yield. The $(Me_2bpb)^{2-}$ ligand frame was strategically chosen for its planarity when bound to the ruthenium center.[21] This allows ample room for binding of the bulky **FlEt** dye trans to NO. Similarly, we also selected the other planar $((OMe)_2IQ1)^{2-}$ ligand frame to isolate [((OMe)$_2$IQ1)Ru(NO)(FlEt)] (**2-FlEt**) from [((OMe)$_2$IQ1)-Ru(NO)(Cl)] (**2-Cl**) using the same synthetic procedure mentioned above.

**Spectroscopic Properties.** The structures of **1-FlEt** and **2-FlEt** have been confirmed with the aid of $^1$H NMR and infrared (IR) spectroscopy, and mass spectrometry (see the Experimental Section). IR spectra of **1-FlEt** and **2-FlEt** (Supporting Information, Figures S1 and S2) reveal the presence of NO and **FlEt**, as evidenced by their NO stretching frequencies ($\nu_{NO}$) at 1846 and 1832 $cm^{-1}$ in addition to their FlEt carbonyl stretching frequencies ($\nu_{CO}$) at 1715 and 1712 $cm^{-1}$, respectively. The greater electron-donating ability of the (OMe)$_2$IQ1 ligand frame causes an increase in electron density in the $\pi^*$ level of the bound NO of **2-FlEt** and is responsible for its lower $\nu_{NO}$ frequency.

Both complexes are diamagnetic and afford clean $^1$H NMR spectra, as expected for $\{RuNO\}^6$ nitrosyls. The integration and number of the peaks observed in both $^1$H NMR spectra confirm the presence of Ru-bound FlEt. For example, in the $^1$H NMR spectrum of free **FlEt**, there are several overlapping aromatic peaks that shift apart upon binding to the Ru center. Thus, none of the 10 aromatic FlEt hydrogen peaks overlap with one another in the $^1$H NMR spectra of **1-FlEt** or **2-FlEt** in $CDCl_3$ (see the Supporting Information, Figures S4 and S5). Similarly, several peaks corresponding to the hydrogen atoms on the ligand frame shift upon metal binding. In addition, there is no evidence of either Cl-bound or free **FlEt** starting materials in either spectrum.

**Electronic Absorption Spectra.** Our pervious studies have shown that the attachment of suitable dye chromophores enhances the visible light absorption of $\{RuNO\}^6$ nitrosyls.[22] In the present work, we have utilized the fluorescein ethyl ester **FlEt** (and not fluoroscein) as the light-harvesting chromophore. The protection of the carboxylate group of fluoroscein (necessary for specific binding to the Ru center of the nitrosyl), however, did not eliminate the visible light absorption by the dye. In its deprotonated form, $FlEt^-$ has an intense absorption band at 504 nm ($\varepsilon$ = 80 000, in 50:50 MeCN/$H_2O$). Interestingly, there is a 50 nm blue shift (to 454 nm) coupled with a reduction in intensity ($\varepsilon$ = 20 000, in MeCN/AcOH) of this absorption band when **FlEt** is in its protonated state (**FlEt-H**, Figure 1). Similar changes in the intensity of the dye band are also observed upon coordination of the dye to the Ru center in **1-FlEt** and **2-FlEt** (Figure 2).


dx.doi.org/10.1021/ic201242d |*Inorg. Chem.* 2011, 50, 9045–9052

The electronic absorbance spectra of **1-FlEt** and **2-FlEt** are very similar, with the main absorption bands of each nitrosyl centered at 475 nm (Figure 2). The extinction coefficient values at 475 nm for these FlEt-bound $\{RuNO\}^6$ nitrosyls are quite high ($\varepsilon$ = 24 000 and 28 000 $M^{-1}$ $cm^{-1}$, respectively). In addition, the general shapes of the absorption bands in both spectra are very similar to that of **FlEt-H**, each containing three overlapping peaks in the visible region. The high $\varepsilon$ values of **1-FlEt** and **2-FlEt** over this large range of wavelengths (400−550 nm) lead to a significant amount of visible light absorption by these dye−nitrosyl conjugates. Indeed, the attachment of **FlEt** in both nitrosyls has significantly enhanced the amount of visible light absorption compared with the corresponding Cl-bound $\{RuNO\}^6$ nitrosyls (Figure 2). For example, the lowest-energy absorbance band in the spectrum of [$(Me_2bpb)Ru(NO)(Cl)$] (**1-Cl**) has a $\lambda_{max}$ at 395 nm with an $\varepsilon$ of 5300 $M^{-1}$ $cm^{-1}$. There is increased visible light absorption in the case of [$((OMe)_2$-IQ1$)Ru(NO)(Cl)$] (**2-Cl**) due to the replacement of the methyl and pyridine substituents (in $Me_2bpb$) with more electron-donating methoxy groups and more conjugated quinoline donors (in $(OMe)_2IQ1$), respectively. Thus, **2-Cl** has a $\lambda_{max}$ at 475 nm with an $\varepsilon$ value of 8700 $M^{-1}$ $cm^{-1}$. Similarly, the increased visible light absorption due to the $(OMe)_2IQ1$ ligand frame also seems to cause an increase in $\varepsilon$ value for **2-FlEt** compared with that of **1-FlEt**.

**Photorelease of NO.** Upon exposure to visible light ($\lambda$ > 465 nm, 300 mW), solutions of **1-FlEt** and **2-FlEt** in solvents, such as MeCN, DMF, $H_2O$, and PBS buffer, undergo similar rapid changes in their electronic spectra (Figure 3 and Figures S6 and S7, Supporting Information). In addition, no significant changes were observed in the spectra when such solutions were kept in the dark for several hours. Given the known NO photolability of similar $\{RuNO\}^6$ nitrosyls,[14,19] the light-induced absorption changes can be linked to the photorelease of NO (and FlEt, vide infra), which has been confirmed by measurements with a NO-sensitive electrode (Figure 3, inset). Specifically, the formation of a low-energy absorbance band (at 750 and 700 nm in the case of **1-FlEt** and **2-FlEt**, respectively) is indicative of the formation of a Ru(III) photoproduct upon NO release in both aqueous and nonaqueous solvents. Such transitions have previously been assigned as ligand-to-metal charge-transfer (LMCT) bands for the Ru(III) photoproducts of structurally related ruthenium nitrosyls.[28] Monitoring the rate of increase of these low-energy absorbance bands upon light exposure allows determination of quantum yield values ($\phi$) of NO release for these $\{RuNO\}^6$ nitrosyls. Comparison of the these quantum yield values (measured in DMF for comparison with previously synthesized nitrosyls) reveals an increased efficiency of NO

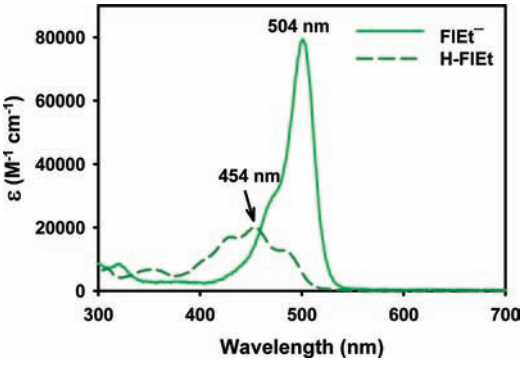


**Figure 1.** Electronic absorption spectra of fluorescein ethyl ester (**FlEt**, in 50:50 MeCN/$H_2O$) and protonated **FlEt-H** (in MeCN/AcOH pH = 5).

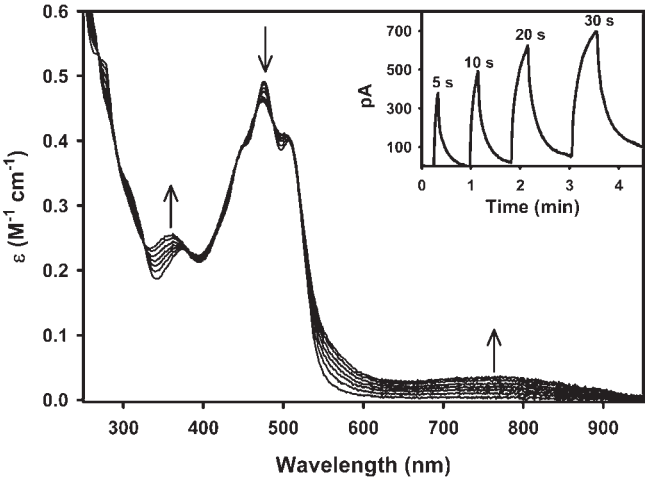


**Figure 3.** Changes in the electronic absorption spectrum upon photolysis of **1-FlEt** in MeCN following illumination with visible light. Inset: NO amperogram of **1-FlEt** in 50:50 MeCN/$H_2O$ upon illumination with visible light for time periods (in seconds) as indicated.

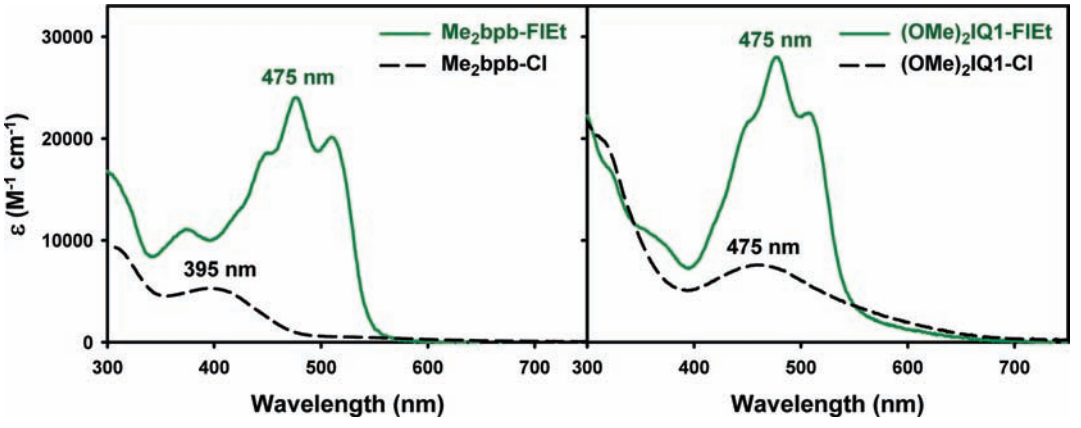


**Figure 2.** Electronic absorption spectra of [$(Me_2bpb)Ru(NO)(Cl)$] and [$(Me_2bpb)Ru(NO)(FlEt)$] (left panel) and [$((OMe)_2IQ1)Ru(NO)(Cl)$] and [$((OMe)_2IQ1)Ru(NO)(Cl)$] (right panel) in MeCN.


dx.doi.org/10.1021/ic201242d |*Inorg. Chem.* 2011, 50, 9045–9052

**Table 1. Summary of Absorption Parameters ($\lambda_{max}$, $\varepsilon$) and Quantum Yield ($\phi$) Values of NO Release from Selected Dye−Nitrosyl Conjugates**

| complex | quantum yield $\phi$ ($\lambda_{irr}$, nm) | solvent | $\lambda_{max}$, nm ($\varepsilon$, $M^{-1}$ $cm^{-1}$) |
|---|---|---|---|
| $[(Me_2bpb)Ru(NO)(Cl)]$ (**1-Cl**) [a] | 0.0008 ± 0.0002 (500) | DMF | 395 (5300) |
| $[(Me_2bpb)Ru(NO)(Resf)]$ (**1-Resf**)[b] | 0.052 ± 0.008 (500) | DMF | 500 (11 920) |
| $[(Me_2bpb)Ru(NO)(FlEt)]$ (**1-FlEt**) | 0.306 ± 0.01 (500) | DMF | 475 (24 000) |
| $[((OMe)_2IQ1)Ru(NO)(Cl)]$ (**2-Cl**)[a] | 0.035 ± 0.005 (500) | DMF | 475 (8700) |
| $[((OMe)_2IQ1)Ru(NO)(Resf)]$ (**2-Resf**)[b] | 0.271 ± 0.008 (500) | DMF | 500 (31 000) |
| $[((OMe)_2IQ1)Ru(NO)(FlEt)]$ (**2-FlEt**) | 0.173 ± 0.01 (500) | DMF | 475 (28 000) |
| Roussin's salt ester (RSE)[c] | 0.00019 ± 0.00005(546) | $CHCl_3$ | 364 (8500) |
| Fluor-RSE[d] | 0.0036 ± 0.0005(436) | $MeCN/H_2O$ | 506 (72 200) |

[a] Reference 21. [b] Reference 22. [c] Reference 29. [d] Reference 25.

release for the FlEt-bound nitroyls (**1** and **2**) compared with their parent Cl-bound nitrosyls (**1-Cl** and **2-Cl**; see Table 1). For example, exposure of **1-Cl** to 500 nm light results in a very low quantum yield ($\phi_{500}$) value of 0.0008, whereas a similar light exposure of **1-FlEt** leads to a significantly larger $\phi_{500}$ value of 0.30. Interestingly, **1-FlEt** has a larger $\phi_{500}$ compared with that of **2-FlEt** ($\phi_{500}$ = 0.17). The opposite is true in the case of the corresponding Resf-tethered $\{Ru\text{-}NO\}^6$ nitrosyls. For example, the $\phi_{500}$ value of the Resf-bound nitrosyls $[(OMe)_2IQ1)Ru(Resf)]$ (**2-Resf**)[21] is larger than that of $[(Me_2bpb)Ru(Resf)]$ (**1-Resf**, Table 1).[22] Comparison of the extinction coefficient ($\varepsilon$) values at 500 nm of **1-Resf** ($\varepsilon$ = 11 920 $M^{-1}$ $cm^{-1}$) and **2-Resf** ($\varepsilon$ = 31 000 $M^{-1}$ $cm^{-1}$) suggests that the increased absorption at 500 nm for **2-Resf** (compared to **1-Resf**) could account for its larger $\phi_{500}$ value. However, the same is not true for the FlEt-tethered nitrosyls. Despite similar extinction coefficient values, **1-FlEt** ($\varepsilon_{500}$ = 19 000 $M^{-1}$ $cm^{-1}$) exhibits a higher $\phi_{500}$ value than **2-FlEt** ($\varepsilon_{500}$ = 22 000 $M^{-1}$ $cm^{-1}$). The latter observation indicates that increased absorption of light cannot be the only reason for the enhanced NO photorelease. The reason for the accelerated NO release upon illumination, therefore, awaits more experimental and theoretical investigation. Such investigation is in progress at this time.

**Fluorescence Turn-ON.** Given the intense fluorescence of free fluorescein, we were interested to see if **1-FlEt** and **2-FlEt** also had fluorescent properties. Because the ethyl ester fluorescein derivative was used for these nitroyls, we first examined the fluorescent properties of **FlEt**. The conversion of fluorescein into **FlEt** results in a small decrease in its fluorescence quantum yield ($\phi_{fl}$ = 0.93 and 0.77, respectively, Table 2).[25] However, upon direct coordination of **FlEt** to the $\{RuNO\}^6$ center in both **1-FlEt** and **2-FlEt**, the fluorescence is almost completely quenched ($\phi_{fl}$ = 0.009 and 0.017, respectively). Interestingly, there is a rapid increase in the fluorescence of solutions of **1-FlEt** and **2-FlEt** in 50:50 $MeCN/H_2O$ upon exposure to light (NO photorelease). In addition, the residual fluorescence observed for solutions of **1-FlEt** and **2-FlEt** becomes completely quenched upon exposure to light in *very dry solvents* (such as MeCN). It is thus evident that these FlEt-bound $\{RuNO\}^6$ nitrosyls are light-activated fluorescence turn-ON agents *only* in the presence of water. Figure 4 shows the increase in fluorescence ($\lambda_{ex}$ = 480 nm, $\lambda_{em}$ = 526 nm) of **1-FlEt** and **2-FlEt** (in 50:50 $MeCN/H_2O$) observed after 1 min intervals of visible light exposure. There is a 27-fold fluorescence turn-ON for **1-FlEt** after 5 min of light exposure. In the case of **2-FlEt**, there is a 5-fold fluorescence increase under similar conditions. These findings follow a similar trend (**1-FlEt** > **2-FlEt**) to that observed

**Table 2. Summary of Absorption and Emission Parameters ($\lambda_{ex}$ = 480 nm) and Fluorescence Quantum Yield ($\phi_{fl}$) Values of Selected Compounds in 50:50 $MeCN/H_2O$ at pH 7**

| compound | absorbance $\lambda_{max}$ | emission $\lambda_{max}$ | fluorescence quantum yield $\phi_{fl}$ |
|---|---|---|---|
| fluorescein | 496 nm | 518 nm | 0.93 ± 0.02 [a] |
| **FlEt** | 504 nm | 526 nm | 0.77 ± 0.02 [b] |
| **1-FlEt** | 475 nm | 526 nm | 0.009 ± 0.002 |
| **2-FlEt** | 475 nm | 526 nm | 0.017 ± 0.003 |

[a] Measured in aqueous solution at pH 11. [b] Measured in a 50:50 mixture of MeCN/phosphate buffer at pH 7.4.

for the NO photolability of **1-FlEt** and **2-FlEt**. Thus, the extent of fluorescence turn-ON correlates with the amount of light-triggered NO release from these $\{RuNO\}^6$ nitrosyls and indicates that the two reactions are intimately connected. Also, the results clearly demonstrate that both NO release and fluorescence turn-ON occurs only upon exposure to light since neither reaction occurs when the solutions of **1-FlEt** and **2-FlEt** (in aqueous or nonaqueous media) are kept in the dark. Although overlap of the dye bands (free and bound, in the range of 400−510 nm) and fluorescence bands (also in the same region) prevents one to *quantitatively* correlate the extent of such turn-ON with the light-triggered NO release in the present case, the dye−nitrosyl conjugates **1-FlEt** and **2-FlEt** do provide turn-ON signals upon NO release that could be effectively utilized in biological systems.

To understand the structural changes responsible for the increase in fluorescence, we have employed $^1H$ NMR spectroscopy to monitor the fate of **1-FlEt** and **2-FlEt** upon light exposure in wet $CDCN_3$. When left in the dark for several hours, there are no changes in the $^1H$ NMR spectra of both nitrosyls. However, exposure of the solutions of **1-FlEt** and **2-FlEt** to visible light results in the appearance of new peaks consistent with those of free **FlEt** (Figure 5 and Figure S8, Supporting Information). The new dye peaks do not show significant line broadening after initial light exposure due to the low concentration of the Ru(III) photoproduct in the solution. However, once the samples have been fully photolyzed, the $^1H$ NMR spectra broaden considerably. In addition, a low-spin Ru(III) EPR signal is observed for such solutions (vide infa). Thus, it becomes clear that the increase in fluorescence observed upon light exposure in water is due to the release of **FlEt** from the Ru(III) photoproduct.

We hypothesize that this release of **FlEt** arises due to the formation of a thermodynamically stable HO-bound Ru(III) photoproduct. When NO is bound, the Ru center is thought to


dx.doi.org/10.1021/ic201242d |*Inorg. Chem.* 2011, 50, 9045–9052

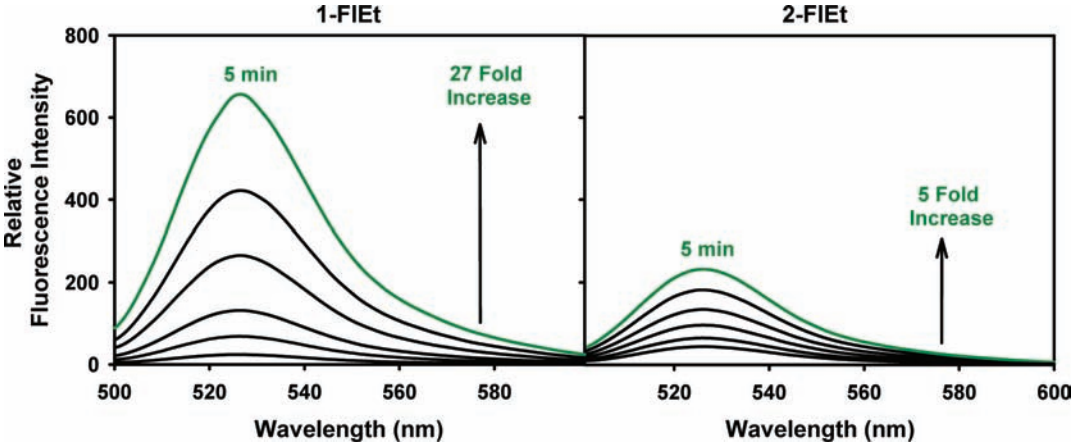


**Figure 4.** Changes in the fluorescence emission spectra upon 1 min intervals of visible light illumination of **1-FlEt** (left panel) and **2-FlEt** (right panel) in 50:50 $H_2O$/MeCN ($\lambda_{ex}$ = 480 nm). Samples with absorbance values of 0.09 at 480 nm were used.

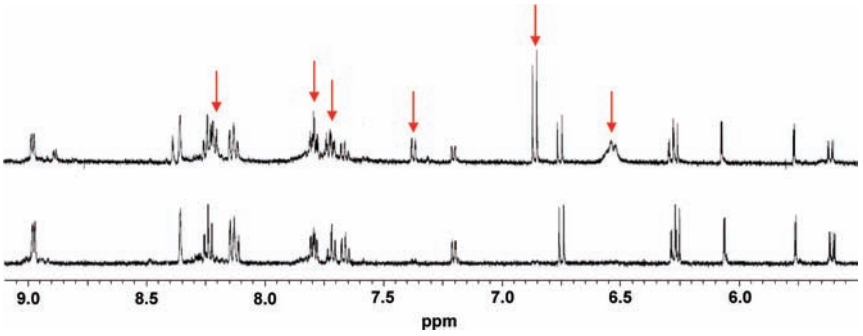


**Figure 5.** Proton NMR spectra (9.1−5.5 ppm) of **1-FlEt** in $CD_3CN$ at 298 K kept in the dark (bottom) and after light exposure (top). The red arrows show new peaks of unbound **FlEt** dye.

have more low-spin Ru(II) character. However, once NO has been released, the Ru center is converted into a low-spin Ru(III) species that is more susceptible to aquation (eq 1). The high Lewis acidity of the resulting water-bound Ru(III) complex combined with the basic properties of $FlEt^-$ may eventually lead to the formation of the more stable $[(L)Ru(III)(OH)(H_2O)]$ (L = $Me_2$bpb or $(OMe)_2$IQ1) photoproduct and **FlEt-H** (eq 2). Indeed, changes in the absorption spectrum of **1-FlEt** upon light exposure in aqueous solvents (Figure S6, Supporting Information) suggest that the free dye ultimately becomes protonated because the intensity of the free dye band is similar to that of the original dye-bound **1-FlEt** absorption band (Figures 1 and 2). If the free dye were fully deprotonated, the intensity of the band would be expected to be much greater since it has a larger extinction coefficient value.

$$[(L)Ru(NO)(FlEt)] \xrightarrow{H_2O} NO^{\bullet} + [(L)Ru^{3+}(H_2O)(FlEt)]^{+} \quad (1)$$

$$[(L)Ru^{3+}(H_2O)(ElEt)]^{+} \xrightarrow{H_2O} [(L)Ru^{3+}(H_2O)(OH)] + FlEt\text{-}H \quad (2)$$

$$(L = Me_2bpb \text{ or} (OMe)_2IQ1)$$

In dry nonaqueous solvents, the **FlEt** dye in **1-FlEt** and **2-FlEt** stays bound to the Ru(III) center upon light exposure and NO release. The small residual fluorescence observed for **1-FlEt** and **2-FlEt** in such solvents is also quenched following the NO loss. However, the resulting paramagnetic low-spin Ru(III) center of the dye photoproducts $[(L)Ru(III)(FlEt)(solv)]$ (L = $Me_2$bpb or $(OMe)_2$IQ1) is responsible for the fluorescence quenching. To confirm the 3+ oxidation state of ruthenium in the solvato species generated after complete photolysis of the diamagnetic $\{Ru\text{-}NO\}^6$ nitrosyls **1-FlEt** and **2-FlEt**, EPR measurements were performed. Photoproducts of **1-FlEt** and **2-FlEt** generated in dry MeCN display axial EPR spectra ($g$ values: 2.16 and 1.89 for **1-FlEt** and 2.18 and 1.90 for **2-FlEt**) typical of low-spin Ru(III). In contrast, the spectra change when photolysis is done in the presence of water ($g$ values: 2.19 and 1.88 for **1-FlEt** and 2.12 and 1.92 for **2-FlEt**). Comparison of the EPR spectra of the photoproduct of **1-FlEt** in aqueous media (Figure S8, Supporting Information) with that of $[(Me_2bpb)Ru(NO)(OH)]$[22] after photolysis under similar conditions confirms such a conclusion (similar spectra with identical $g$ values). Collectively, these results support the hypothesis that the ultimate formation of the OH-bound photoproduct $[(L)Ru(III)(OH)(H_2O)]$ (L = $Me_2$bpb or $(OMe)_2$IQ1) drives the release of **FlEt**.

Previously, we shown that $\{RuNO\}^6$ nitrosyls with coordinated Resf[21,22] or dansyl[30] dye chromophores display *turn-OFF* fluorescence signal once NO is released. The decrease in fluorescence has been attributed to the formation of dye-bound Ru(III) photoproducts. The paramagnetic $d^5$ Ru(III) center is a very effective fluorescence quencher of the bound Resf and


dx.doi.org/10.1021/ic201242d |*Inorg. Chem.* 2011, 50, 9045–9052

Scheme 1

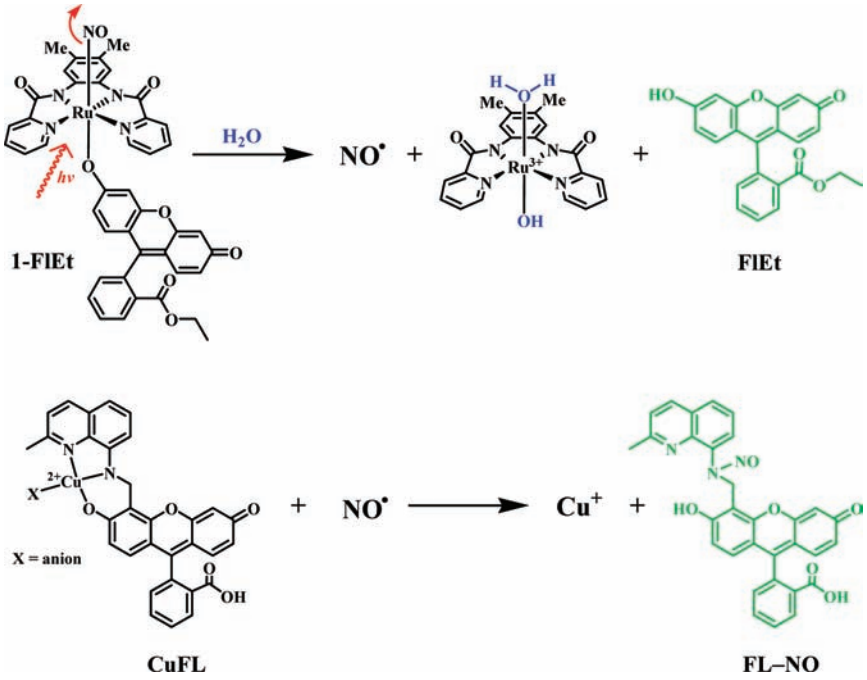


dansyl-imidazole (Ds-im) dyes in these photoproducts. In contrast, **1-FlEt** and **2-FlEt** are the first examples of ruthenium nitrosyls with a fluorescent *turn-ON* signal for NO release. Although a Ru(III) photoproduct is also produced in this case, the **FlEt** dye does not stay bound to the metal center in the presence of water. It becomes apparent that **FlEt** has a lower affinity for Ru(III) compared with that of Resf or Ds-im. Thus, as NO leaves, generating a Ru(III) photoproduct, **FlEt** is released and a fluorescence enhancement is noted instead of quenching (Scheme 1, top).

Recently, there have been several reports of fluorescent turn-ON sensors that signal the presence of NO.[31] For example, Lippard and co-workers have designed a Cu(II) fluorescein-based NO sensor CuFL (FL = 2-{2-chloro-6-hydroxy-5-[(2-methyl-quinolin-8-ylamino)-methyl]-3-oxo-3*H*-xanthen-9-yl}-benzoic acid).[32] The FL ligand is not fluorescent in its free or Cu(II)-bound form. However, upon expose to NO, the Cu(II) center of CuFl is reduced to Cu(I) with concomitant *N*-nitrosylation of FL (FL-NO). The *N*-nitrosylation of the FL-NO ligand results in its displacement from the Cu(I) center and an increase in fluorescence (Scheme 1, bottom). Indeed, CuFL has been successfully used to visualize NO generated from iNOS in murine macrophage cells and from cNOS in SK-N-SH human neuroblastoma cells.[32] However, in the present case, our goal is to deliver exogenous NO to biological targets. With **1-FlEt** and **2-FlEt**, the release of NO (instead of NO binding) results in a fluorescent turn-ON signal that could clearly indicate NO delivery. This is a distinct advantage of the designed NO donors **1-FlEt** and **2-FlEt**. Studies on the utility of these nitrosyls in NO delivery to biological targets are in progress in this laboratory.

## ■ ASSOCIATED CONTENT

**Ⓢ Supporting Information.** FTIR spectra of **1-FlEt** and **2-FlEt** (Figures S1 and S2), $^1$H NMR spectra of free **FlEt**, **1-FlEt**, and **2-FlEt** (Figures S3, S4, and S5), changes in the electronic absorption (Figures S6 and S7) and $^1$H NMR (Figure S8) spectra upon photolysis of **2-FlEt**, and EPR spectrum of the photoproduct of **1-FlEt** in 50:50 MeCN/$H_2O$ (Figure S9). This material is available free of charge via the Internet at http://pubs.acs.org.

## ■ AUTHOR INFORMATION

**Corresponding Author**
*E-mail: pradip@chemistry.ucsc.edu.

## ■ ACKNOWLEDGMENT

Financial support from a grant from the National Science Foundation (CHE-0957251) is gratefully acknowledged. N.L.F. received partial support from a COR-SRG grant from UCSC.

## ■ REFERENCES

(1) Ignarro, L. J. *Nitric Oxide: Biology and Pathobiology*; Academic Press: San Diego, 2000.
(2) Kalsner, S., Ed. *Nitric Oxide Free Radicals in Peripheral Neurotransmission*; Birkhauser: Boston, 2000.
(3) Ko, G. Y.; Fang, F. C. *Nitric Oxide and Infection*; Kluwer Academic/Plenum Publishers: New York, 1999.
(4) Moncada, S., Higgs, E. A., Bagetta, G., Eds. *Nitric Oxide & the Cell: Proliferation, Differentiation and Death*; Portland Press: London, 1998.
(5) Degoute, C. S. *Drugs* **2007**, *67*, 1053–1076.
(6) Fang, F. C. *Nat. Rev. Microbiol.* **2004**, *2*, 820–832.
(7) Fang, F. C. *J. Clin. Invest.* **1997**, *99*, 2818–2825.
(8) Kanwar, J. R.; Kanwar, R. K.; Burrow, H.; Baratchi, S. *Curr. Med. Chem.* **2009**, *16*, 2373–2394.
(9) Hirst, D.; Robson, T. *J. Pharm. Pharmacol.* **2007**, *59*, 3–13.
(10) Xu, W.; Liu, L. Z.; Loizidou, M.; Ahmed, M.; Charles, I. G. *Cell Res.* **2002**, *12*, 311–320.

(11) (a) Rose, M. J.; Mascharak, P. K. *Curr. Opin. Chem. Biol.* **2008**, *12*, 238–244. (b) Eroy-Reveles, A. A.; Mascharak, P. K. *Future Med. Chem.* **2009**, *8*, 1497–1507.
(12) (a) Ford, P. C.; Bourassa, J.; Miranda, K.; Lee, B.; Lorkovic, I.; Boggs, S.; Kudo, S.; Laverman, L. *Coord. Chem. Rev.* **1998**, *171*, 185–202. (b) Patra, A. K.; Afshar, R. K.; Olmstead, M. M.; Mascharak, P. K. *Angew. Chem., Int. Ed.* **2002**, *41*, 2512–2515. (c) Patra, A. K.; Rowland, J. M.; Marlin, D. S.; Bill, E.; Olmstead, M. M.; Mascharak, P. K. *Inorg. Chem.* **2003**, *42*, 6812–6823. (d) Eroy-Reveles, A. A.; Hoffman-Luca, C. G.; Mascharak, P. K. *Dalton Trans.* **2007**, 5268–5274.
(13) (a) Ghosh, K.; Eroy-Reveles, A. A.; Holman, T. R.; Olmstead, M. M.; Mascharak, P. K. *Inorg. Chem.* **2004**, *43*, 2988–2997. (b) Hoffman-Luca, C. G.; Eroy-Reveles, A. A.; Alvarenga, J.; Mascharak, P. K. *Inorg. Chem.* **2009**, *48*, 9104–9111.
(14) Rose, M. J.; Mascharak, P. K. *Coord. Chem. Rev.* **2008**, *252*, 2093–2114.
(15) (a) Bigio, I. J.; Bown, S. G. *Cancer Biol. Ther.* **2004**, *3*, 259–267. (b) Dolmans, D. E. J. G.; Fukumura, D.; Jain, R. K. *Nat. Rev. Cancer* **2003**, *3*, 380–387.
(16) Levina, A.; Mitra, A.; Lay, P. A. *Metallomics* **2009**, *1*, 458–470.
(17) Tfouni, E.; Krieger, M.; McGarvey, B. R.; Franco, D. W. *Coord. Chem. Rev.* **2003**, *236*, 57–69.
(18) Cox, A. B.; Wallace, R. N. *Inorg. Nucl. Chem. Lett.* **1971**, *7*, 1191–1194.
(19) (a) Fry, N. L.; Mascharak, P. K. *Acc. Chem. Res.* **2011**, *44*, 289–298. (b) Tfouni, E.; Doro, F. G.; Figueiredo, L. E.; Pereira, J. C. M.; Metzker, G.; Franco, D. W. *Curr. Med. Chem.* **2010**, *17*, 3643–3657.
(20) Patra, A. K.; Rose, M. J.; Murphy, K. M.; Olmstead, M. M.; Mascharak, P. K. *Inorg. Chem.* **2004**, *43*, 4487–4495.
(21) Fry, N. L.; Heilman, B. J.; Mascharak, P. K. *Inorg. Chem.* **2011**, *50*, 317–324.
(22) (a) Rose, M. J.; Olmstead, M. M.; Mascharak, P. K. *J. Am. Chem. Soc.* **2007**, *129*, 5342–5343. (b) Rose, M. J.; Fry, N. L.; Marlow, R.; Hink, L.; Mascharak, P. K. *J. Am. Chem. Soc.* **2008**, *130*, 8834–8846.
(23) Smith, L. M.; Sanders, J. Z.; Kaiser, R. J.; Dodd, C.; Connell, C. R.; Heiner, C.; Kent, S. B. H.; Hood, L. E. *Nature* **1986**, *321*, 674–679.
(24) Nolan, E. M.; Jaworski, J.; Okamoto, K.; Hayashi, Y.; Sheng, M.; Lippard, S. J. *J. Am. Chem. Soc.* **2005**, *127*, 16812–16823.
(25) Wecksler, S. R.; Hutchinson, J.; Ford, P. C. *Inorg. Chem.* **2006**, *45*, 1192–1200.
(26) (a) Schmidt, R.; Brauer, H. D. *J. Photochem.* **1984**, *25*, 489–499. (b) Murov, S. *Handbook of Photochemistry*; Marcel Dekker: New York, 1973.
(27) Lakowicz, J. R. *Principles of Fluorescence Spectroscopy*, 2nd ed.; Kluwer Academic/Plenum: New York, 1999.
(28) (a) Works, C. F.; Ford, P. C. *J. Am. Chem. Soc.* **2000**, *122*, 7592–7593. (b) Bordini, J.; Hughes, D. L.; Da Motta Neto, J. D.; da Cunha, J. C. *Inorg. Chem.* **2002**, *41*, 5410–5416.
(29) Bourassa, J.; DeGraff, W.; Kudo, S.; Wink, D. A.; Mitchell, J. B.; Ford, P. C. *J. Am. Chem. Soc.* **1997**, *119*, 2853–2860.
(30) Rose, M. J.; Mascharak, P. K. *Chem. Commun.* **2008**, 3933–3935.
(31) (a) McQuade, L. E.; Lippard, S. J. *Curr. Opin. Chem. Biol.* **2010**, *14*, 43–49. (b) Lim, M. H.; Lippard, S. J. *Acc. Chem. Res.* **2007**, *40*, 41–51.
(32) Lim, M. H.; Xu, D.; Lippard, S. J. *Nat. Chem. Biol.* **2006**, *2*, 375–380.